

# Effect of high loading of titanium dioxide particles on the morphology, mechanical and thermo-mechanical properties of the natural rubber-based composites

Janusz Datta<sup>1</sup>  · Paulina Kosiorek<sup>1</sup> · Marcin Włoch<sup>1</sup>

Received: 5 May 2016 / Accepted: 1 November 2016 / Published online: 7 November 2016  
© The Author(s) 2016. This article is published with open access at Springerlink.com

**Abstract** The aim of this work was to prepare and characterize the natural rubber vulcanizates containing different amounts of titanium dioxide particles. At first, a rubber mixture was prepared using a laboratory two-roll mill and then samples were vulcanized by a hydraulic press. The formulation of the rubber mixture and rubber-processing technique were based on our earlier investigations. Samples were obtained with different titanium dioxide loadings of 15, 25, 45, and 85 parts by weight per hundred parts of natural rubber. This research is focused on the determination of the influence of different loadings of titanium oxide particles on the chemical structure, morphology, mechanical and thermo-mechanical properties of the natural rubber-based composites. It was found that vulcanizates with different amounts of TiO<sub>2</sub> particles possess good characteristic in terms of all measured properties. The results of Fourier transform infrared spectroscopy analysis showed that the chemical structure of the obtained natural-based composites was not influenced by titanium dioxide particles. The SEM micrographs showed the uniform dispersion of TiO<sub>2</sub> particles in the natural rubber matrix. The agglomeration of filler was seen at the higher contents of TiO<sub>2</sub> in the matrix. The thermogravimetric analysis showed slightly different thermal stability for the obtained natural rubber composites. The dynamic mechanical thermal analysis showed that the prepared materials have similar glass transition temperatures. However, increase in the content of titanium dioxide in the obtained materials is connected with higher energy

loss (higher dissipation of energy) during the mechanical work of material and higher cross-link density of the prepared materials.

**Keywords** Natural rubber composites · Titanium dioxide · Mechanical properties · Dynamic mechanical properties · Thermal stability · Swelling properties

## Introduction

Natural or synthetic rubber-based composites with inorganic fillers possess increasing importance from the technological point of view [1, 2]. The practical applications are determined by achievement of desirable mechanical and dynamic properties of rubber-based materials, which is connected with the optimal degree of cross-linking in the rubber vulcanizates. The cross-link density should be high enough to prevent viscous flow, but low to avoid brittle failure of the vulcanizates materials [3]. Rubber materials are commonly used for the production of o-rings, seals, tires or conveyor belts [4].

There are many kinds of rubbers, such as butadiene rubber (BR), ethylene-propylene-diene monomer rubber (EPDM), nitrile-butadiene rubber (NBR) [5], styrene-butadiene rubber (SBR), and natural rubber (NR) [5–8]. Natural rubber shows sufficient tensile strength; tear strength and abrasion resistance for many applications [4, 8]. On the other hand, NR is an unsaturated polymer, sensitive to oxidation initiated by heat, ultraviolet or gamma radiation [8]. The properties of NR and its products can be enhanced by the addition of different types of antioxidants, such as benzophenone, benzotriazole, and amines [8, 9]. The organic antioxidants are unstable and toxic while inorganic ones are generally nontoxic and chemically stable under high temperature and UV irradiation [8, 10].

✉ Janusz Datta  
janusz.datta@pg.gda.pl

<sup>1</sup> Department of Polymers Technology, Faculty of Chemistry, Gdańsk University of Technology, G. Narutowicza Str. 11/12, 80-233 Gdansk, Poland

Fillers are incorporated into rubber compounds to improve processability, cost reduction, and physical properties modifying the composites [11, 12]. One of the most important reasons for filler addition is related to make the production of the final product more economical [11].

In recent years, several inorganic and organic fillers were proposed, i.e., silanes [7, 13], unmodified and modified silica [14, 15], carbon nanotubes [2], carbon black [3, 13], starch, cellulose [16], titanium dioxide, zinc oxide [17, 18], magnesium hydroxide [19], silver nanoparticles [20], wood flour and other lignocellulosic fibers [21].

It is well known that the filler dispersion and filler–rubber interaction are two critical factors, which determine the performance of the composites [1, 22]. Other factors are structure, size, shape, surface area and surface reactivity of the filler particles [22–24].

Titanium dioxide is widely used as filler in polymer matrix composites. It is resulted from its useful properties, e.g., low-cost and high-effective pigment, high surface area per particle size connected with good effectiveness in UV protection [8, 25]. Titanium dioxide is also a safe material for human and animals and possesses photocatalytic and bactericidal effects [25, 26]. Moreover, it was found that  $\text{TiO}_2$  particles can improve physical and mechanical properties of the polymeric materials [11]. Literature review is also shown that  $\text{TiO}_2$  particles have free surface hydroxyl groups, and this fact caused a small tendency for aggregation but good dispersion of the  $\text{TiO}_2$  in the polymer composites [11, 27]. Hayeemasae et al. [11] reported that the tensile strength of nano-sized  $\text{TiO}_2$  filled natural rubber-based composites is higher than that of the micro-sized  $\text{TiO}_2$  filled NR composites. The highest tensile strength was found at 6 phr of nano and micro-sized  $\text{TiO}_2$  particles. Furthermore, the authors have found that the tensile modulus of the nano-sized  $\text{TiO}_2$  filled NR composite is slightly higher than that of the micro-sized one. This effect is probably caused by the smaller size of the nano-sized  $\text{TiO}_2$  particles resulted in their higher contact surface area. From others works it is known that the modulus is also related to the hardness of the filler [28].

Seentrakoon et al. [8] described natural rubber composites modified by rutile- $\text{TiO}_2$  nanoparticle [abbreviated as n- $\text{TiO}_2$  (R)] and micro particles. The authors showed that addition of 5 phr n- $\text{TiO}_2$ (R) caused improvement in mechanical properties. Higher addition of mentioned n- $\text{TiO}_2$ (R) particles resulted in decreasing of the properties. It was also presented that mechanical properties of the composites with 5 phr of micro- $\text{TiO}_2$ (R) were lower than that of the composites with nano- $\text{TiO}_2$ (R). It was also found that addition of n- $\text{TiO}_2$  improved the mechanical properties of the NR composites after UV irradiation. Seentrakoon

et al. [8, 25] concluded that it is resulted from interfacial interaction between applied fillers and rubber matrix. The same facts about  $\text{TiO}_2$  effectiveness in protecting UV was showed by other authors. A lot of investigations confirm that  $\text{TiO}_2$  particles can be used as the anti-aging agent for synthetic and NR-bases materials [18, 25].

Another filler that is frequently used is silica, an excellent nonblack reinforcing filler [13]. But unfortunately it has lower compatibility with non-polar natural rubber due to its polar surface resulted from the presence of silanol groups. Some of the silica surface modification methods for improving the dispersion of silica in the rubber matrix are described in the literature [1, 13]. One of method was proposed by Zhong et al. [1] which explored the effect of silane modified silica (m-silica) on the performance of SBR-based composites. In the first step, they obtained ethylene thiourea-modified silica (silica-s-ETU) by the surface modification of silica using vulcanization accelerator, i.e., ethylene thiourea. The results showed that silica-s-ETU/SBR composites are characterized by filler dispersion and higher mechanical properties than m-silica/SBR composites. Ahmed et al. [22] investigated the natural rubber composites filled with marble sludge (MS) and silica and reported that the addition of silica has more positive effect on the mechanical properties (e.g., tensile strength, modulus, tear strength and hardness) than marble sludge.

In the most cases, the fillers are used to reinforce rubber materials. However, rubber usually works in the dynamic conditions, but the rubber products possess a low-thermal conductivity which causes local generation and accumulation of heat. This problem can be also solved by adding fillers, such as stainless steel fiber, nano-zinc oxide [29], and carbon nanotubes [30] that enhance the thermal conductivity of the final materials.

In the presented work, natural rubber composites were prepared using titanium dioxide as filler. The main purpose of this work was to determine the effect of high filler content on the morphology and selected properties of the obtained natural rubber composites. Additionally, we have examined the effect of vulcanization time (10–25 min) on the properties of the obtained natural rubber-based composites. It is well known that titanium dioxide is cheap inorganic filler which can be applied as a reinforcing agent and cost-reductive additive. The mechanical properties were analyzed in the context of tensile properties, hardness, abrasion resistance, tear strength, cyclic compression behavior and rebound resilience. The dynamic mechanical properties (i.e., storage and loss modulus and damping factor vs. temperature) and thermal stability were also determined and analyzed.

**Table 1** Formulations data of the prepared composites

Ingredients	Quantities (parts per hundred parts of natural rubber)				
	VNR	VNR15	VNR25	VNR45	VNR85
Natural rubber	100	100	100	100	100
Stearic acid	3	3	3	3	3
Zinc oxide	5	5	5	5	5
Stabilizer AR <sup>a</sup>	1,5	1,5	1,5	1,5	1,5
Accelerator T <sup>b</sup>	0,5	0,5	0,5	0,5	0,5
Machine oil	2,5	2,5	2,5	2,5	2,5
TiO <sub>2</sub>	–	15 (11.5 wt%) <sup>c</sup>	25 (17.8 wt%) <sup>c</sup>	45 (28.0 wt%) <sup>c</sup>	85 (42.4 wt%) <sup>c</sup>
Sulfur	3	3	3	3	3

<sup>a</sup> *N*-phenyl- $\beta$ -naphthylamine

<sup>b</sup> Tetramethylthiuramdisulphide (TMTD)

<sup>c</sup> Percentage weight content of titanium dioxide particles in the prepared composites

## Experimental

### Materials

The natural rubber used for preparing composites was supplied by TORIMEX (Poland). Stearic acid, sulfur powder and zinc oxide (POCh AVANTOR, Poland), stabilizer AR (CHMES, Poland), accelerator T (STANDARD, Poland), and oil machine (Nytex 810, Nynas, Poland) were other ingredients used during preparation of the rubber mixture. Titanium dioxide particles (Easy Chem, Poland) was used at the loading of 15, 25, 45, 85 parts by weight per hundred parts of natural rubber. The rubber mixture formulations are shown in Table 1. Titanium dioxide particles have approximate length of  $5.86 \pm 1.25 \mu\text{m}$  and width  $0.98 \pm 0.21 \mu\text{m}$ .

### Preparation of rubber composites

The mixtures of natural rubber, ingredients, and titanium dioxide particles were prepared on the laboratory two-roll mill during 15 min. The ingredients were added in sequence presented in Table 1. The addition of each subsequent component follows good distribution of the earlier component. The rubber compounds were vulcanized by compression molding using a hydraulic press at 145 °C with a pressure of 4–4.5 MPa at four various times of 10, 15, 20 and 25 min.

### Testing methods

#### FTIR

The chemical structures of the obtained natural rubber composites with titanium dioxide and natural rubber without TiO<sub>2</sub> (reference sample) were investigated by means of Fourier transform infrared spectroscopy (FTIR) using a

Nicolet FTIR 8700 spectrophotometer (Thermo Electron Co., USA). The spectra were registered at room temperature for wavenumbers between 500 and 4500 cm<sup>-1</sup> at nominal resolution 4 cm<sup>-1</sup>. Each spectrum was acquired with 64 scans.

#### SEM

The morphology of the cross-sections of prepared materials was determined using a Phenom G2 PRO scanning electron microscope (SEM, Phenom World, The Netherlands). The micrographs were prepared using desktop scanning electron microscope with accelerating voltage of 5 kV. Morphologies were obtained with several magnifications to observe dispersion of filler and its interaction with the natural rubber matrix.

#### Swelling parameters

The determination of all presented swelling parameters is described in the literature in the case of natural rubber composites filled with particulate and fibrous fillers [31–33]. The samples for test were cut from the compression molded sheets (obtained during the vulcanization process of the prepared natural rubber mixtures) and three samples (with the average mass equal ca. 1 g) from each composite type were tested. The prepared composites samples were immersed in toluene at room temperature for 120 h to reach diffusion equilibrium (to obtain constant mass of immersed samples). Then samples were taken out from the solvent and adhered solvent was carefully removed using blotting paper, and mass of each sample was measured. After that the samples were dried in air for six days and in a laboratory oven at 80 °C to the moment when the constant weight was obtained. This procedure was the same as the one we used in the case of natural rubber composites filled with short jute fibers [32].

The swelling ratio (SR) is a mass of a solvent ( $m_{as}$ ), i.e., toluene which was absorbed by the sample divided by the initial mass of the sample ( $m_{is}$ ). The mass of absorbed toluene was determined as difference between the mass of sample after ( $m_{ss}$ ) and before swelling test ( $m_{is}$ ). The swelling ratio was determined using Eq. (1) as follows:

$$SR = \frac{m_{ss} - m_{is}}{m_{is}} = \frac{m_{as}}{m_{is}} \quad (1)$$

The equilibrium swelling method (using the Flory–Rehner relationship, Eq. (2)) was used to determine the cross-link densities ( $\nu$ ) of the prepared natural rubber composites. Other swelling parameters, i.e., volume fraction of the rubber network in the swollen phase ( $V_r$ ) and average molecular weight of the polymer between cross-links ( $M_c$ ) were also determined as follows.

$$\nu = \frac{-\ln(1 - V_r) - V_r - \chi \cdot V_r^2}{V_s \cdot \left( V_r^{\frac{1}{3}} - \frac{1}{2} \cdot V_r \right)} = \frac{1}{M_c} \quad (2)$$

where,  $V_s$  is the molar volume of toluene ( $V_s = 106.52 \text{ cm}^3/\text{mol}$ ),  $\chi$  is the Flory–Huggins natural rubber–toluene interaction constant ( $\chi = 0.38$ ).

#### Static tensile test

Tensile properties, including tensile strength, elongation-at-break, and modulus at 100% and 300% elongation were measured using a universal testing machine Zwick/Roell Z020 (Zwick, Germany) with cross-head speed  $200 \text{ mm min}^{-1}$ , at the temperature  $21 \text{ }^\circ\text{C}$  according to ISO 37. The test samples were prepared in a standard dumbbell shape. The recorded results are averages of five independent measurements.

#### Tear strength

Tear strength was investigated with using a universal testing machine Zwick/Roell Z020 (Zwick, Germany), with cross-head speed  $100 \text{ mm min}^{-1}$  according to ISO 34-1. The test samples were prepared in a crescent shape with nick depth of 1 mm, and all measurements were repeated five times.

#### Cyclic compression and hysteresis

The cyclic compression tests were carried out using a universal testing machine Zwick/Roell Z020 (Zwick, Germany). The cylindrical specimens (diameter = 7 mm and

length = 24 mm) were submitted to five compression-decompression cycles at 50% of their original height and velocity of  $0.7 \text{ mm min}^{-1}$ .

#### Abrasion resistance

The abrasion resistance of the obtained natural rubber composites was determined using a Schopper–Schlobach apparatus (Germany). The recorded results are presented as volume loss of the sample, in accordance with ISO 4649. For each prepared materials three independent tests were taken.

#### Density

Density was measured using an analytical balance RAD-WAG (Poland) by hydrostatic method with using methanol as an immersion medium, in accordance with ISO 2781, at room temperature and measurement was repeated five times for each prepared material.

#### Hardness

Hardness was determined according to ISO 868 standard using an electronic Shore type A (Zwick, Germany) and presented results are average from random ten points in one specimen.

#### Rebound resilience

Rebound resilience (elasticity) was investigated according to ISO 4662 standard. The measurements were carried out using a Schob type rebound tester, and the results are averages of ten independent tests.

#### Dynamic mechanical thermal analysis

Dynamic mechanical analysis (DMA) was carried out using a DMA Q800 analyzer (TA Instruments, USA) according to ASTM D6045, in a temperature range from  $-100$  to  $+150 \text{ }^\circ\text{C}$  at an operating frequency of 1 Hz and heating rate of  $4 \text{ }^\circ\text{C min}^{-1}$  under air atmosphere. The samples dimensions were 2 mm thick, 10 mm wide and 40 mm long. The variation of storage modulus, loss modulus and tangent delta vs. temperature was determined.

#### TGA

Thermogravimetric analysis (TGA) was carried using a NETZSCH analyzer (TG 209F3, Netzsch, Germany). The samples were heated from  $25$  to  $600 \text{ }^\circ\text{C}$  at a rate of  $20 \text{ }^\circ\text{C min}^{-1}$  under nitrogen atmosphere.

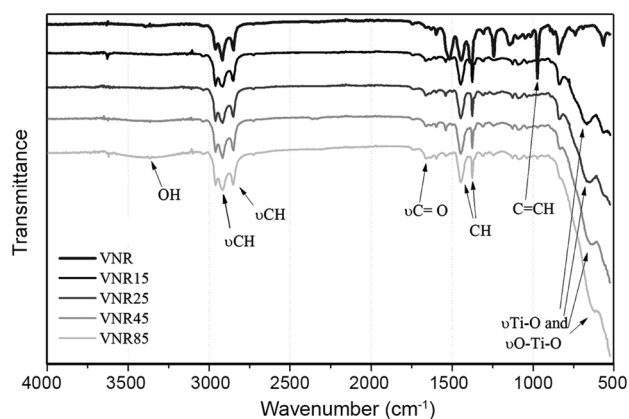


**Fig. 1** FTIR spectra of the obtained natural rubber-based composites

## Results and discussion

### FTIR analysis

Chemical structure of the prepared natural rubber composites were confirmed by FTIR method and shown in Fig. 1. The analysis was performed for all materials. In all types of composites, samples with quite similar spectra were recorded which contain the bands assigned to CH<sub>2</sub> symmetric and asymmetric stretching vibrations (2849–2916 cm<sup>-1</sup>) which were presented as a double peak, also is visible peak connected with CH<sub>3</sub> asymmetric stretching vibration (2958 cm<sup>-1</sup>). The similar results were presented by Seentrakoon et al. [8].

The band at around 1660 cm<sup>-1</sup> indicate the vibration of a hydrogen-bonded C=O group, which is seen only for the filled rubber composites. Probably, the peak is related to the oxidation phenomena that occurred in the rubber matrix after the addition of TiO<sub>2</sub>, which is known as an oxidative agent [8, 34]. It was observed the additional peak at 3370 cm<sup>-1</sup> with increasing of TiO<sub>2</sub> in the composite, which is assigned to the hydroxyl groups on the TiO<sub>2</sub> particles surface. This peak can be observed for VNR45 and VNR85, but in the case of lower loadings of TiO<sub>2</sub>, it is not significant and for natural rubber vulcanizates, it is completely invisible. According to the literature, the peak of the hydroxyl groups on the TiO<sub>2</sub> particles is emerged in the range of 3200–3600 cm<sup>-1</sup> [35].

The unfilled composites exhibit the band at 970 cm<sup>-1</sup>, assigned to C=CH deformation vibration [8] which disappeared after TiO<sub>2</sub> addition into the rubber matrix. Also, this peak was appeared at the same time when the new band appeared at around 1400 cm<sup>-1</sup> which is associated with the bending vibration of CH group. Additionally, we can see the broad and strong peak at approximately 600 cm<sup>-1</sup>, ascribed the absorption band of Ti–O and O–Ti–O flexural vibrations [35, 36]. The VNR sample also exhibited the

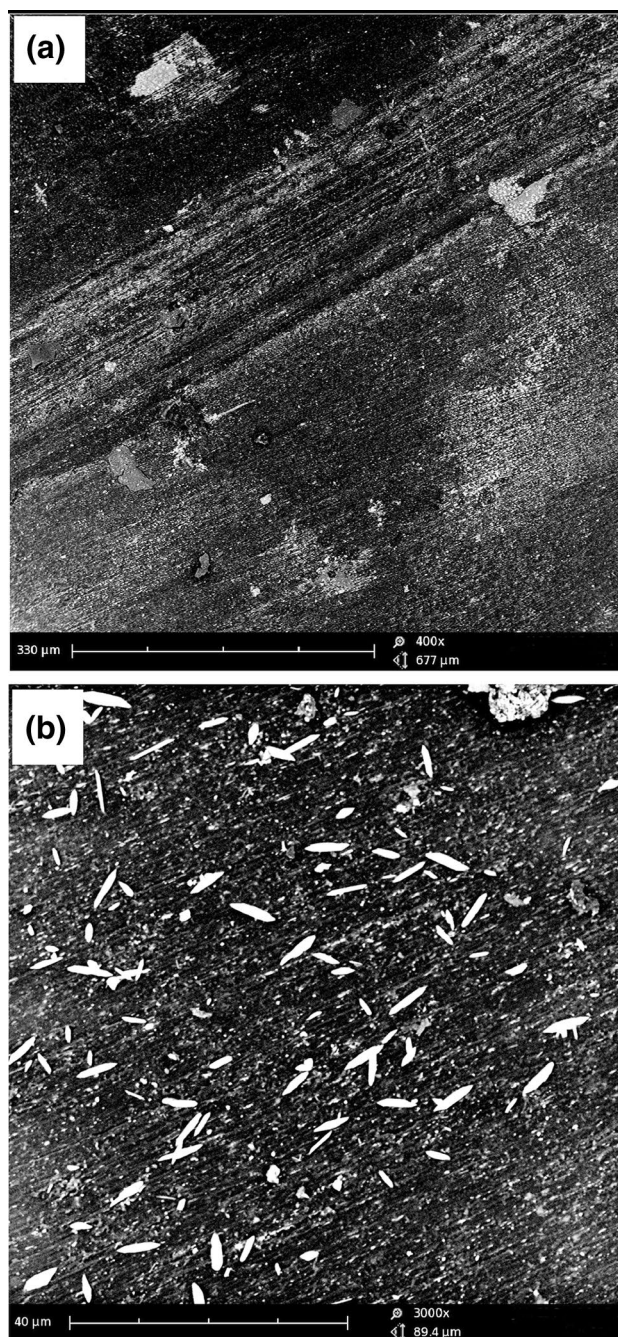


**Fig. 2** SEM micrographs of VNR15

band at 970 cm<sup>-1</sup>, assigned to C=CH deformation vibration [8].

Moreover, with increase in TiO<sub>2</sub> loading in the prepared composites the mentioned peaks became wider and stronger as can be seen for VNR15–VNR85 samples. The results of FTIR analysis confirmed the presence of hydroxyl groups on the surface of the composites materials, therefore in accordance with the current state of knowledge, higher amount of hydroxyl groups on the surface

may result in the improvement of hydrophilic nature of the composites surface [35].

### Morphology study

The obtained SEM micrographs are shown in Figs. 2, 3, 4, 5. Generally, uniform dispersion of  $\text{TiO}_2$  in the natural rubber matrix is observed. However, the fillers tend to form agglomerates at higher loading. It is well known that good dispersion of the filler in the matrix is considered as a main factor to achieve good mechanical properties. The use of higher magnification allows observing the single  $\text{TiO}_2$  particle characterized by the longitudinal shapes. In Figs. 4 and 5,  $\text{TiO}_2$  particles agglomeration can be seen, which the largest ones were observed for the VNR85 sample. It is known that the ability to agglomerate is heightening with increasing the loading of fillers.

### Swelling parameters study

Swelling ratio (SR) decreasing with increasing content of titanium dioxide particles (as seen in Table 2), and this is resulted from the restricted possibility of toluene penetration in natural rubber composites. The restriction of swelling is connected with the presence of particulate filler (titanium dioxide absorb a much less amount of toluene than cross-linked natural rubber) and its interaction with natural rubber. Similar trend was observed by Ahmed et al. [31] in the marble sludge/natural rubber composites. Also, in the case of bio-based fibers similar behavior was observed, for example, in the natural rubber composites filled with short jute [32] and hemp [33] fibers.

The equilibrium swelling measurements permit to determine the cross-link densities of the prepared composites. The cross-link densities of the samples were determined using the Flory–Rehner relationship (measurements were performed in toluene) and this parameter is inversely proportional to the average molecular weight between the cross-links in the composite materials. Results from equilibrium swelling measurements are presented in Table 2. The increase in the amount of  $\text{TiO}_2$  particles in the NR matrix results in the increasing of the cross-link density and decreasing of the average molecular weight between cross-links. This behavior is straightly related to the good interaction between surface of applied particulate filler and natural rubber matrix. The interaction between  $\text{TiO}_2$  particles and polymer chains causes restriction of natural rubber chains mobility, and the penetration of toluene through the NR matrix is hindered.

The increasing of cross-link density influences on the mechanical and thermal properties of the prepared materials, and it will be discussed in detail in the further parts of this work. The increasing of cross-link density with

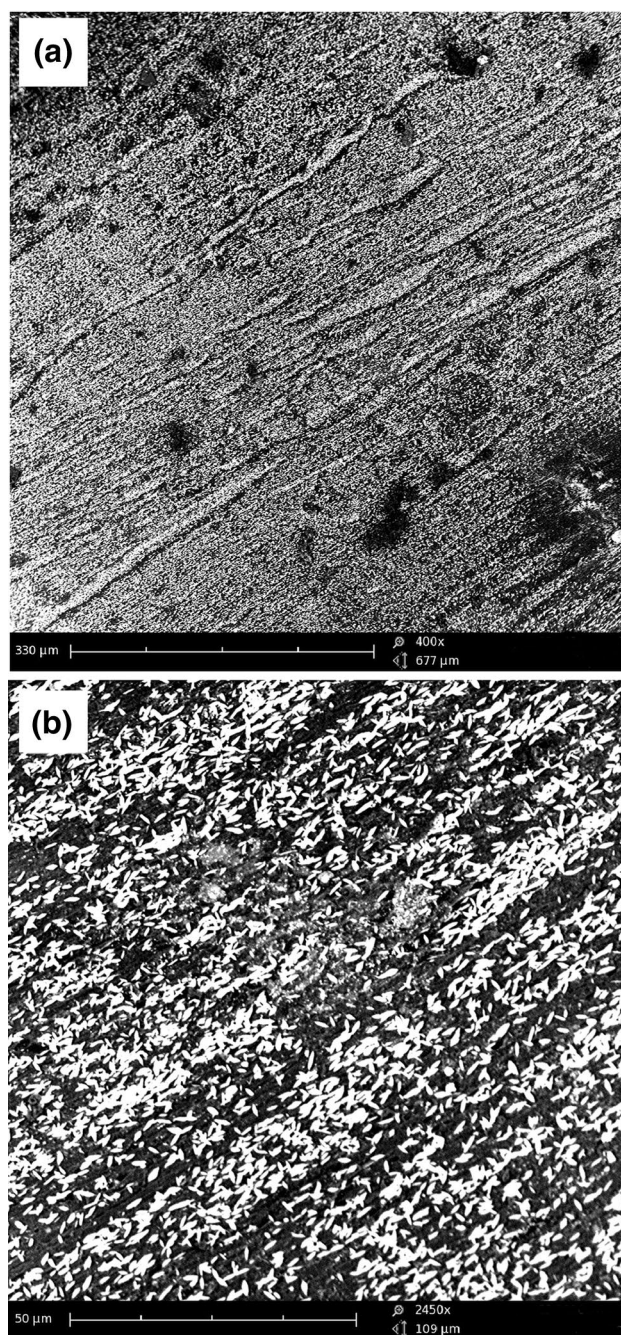


**Fig. 3** SEM micrographs of VNR25

increasing content of the particulate or fibrous filler was observed by other authors, with marble sludge [31], short jute fibers [32] and hemp fibers [33] in the natural rubber composites.

### Static tensile test

The results from static tensile test are shown in Table 3. The natural rubber vulcanizates possess the highest

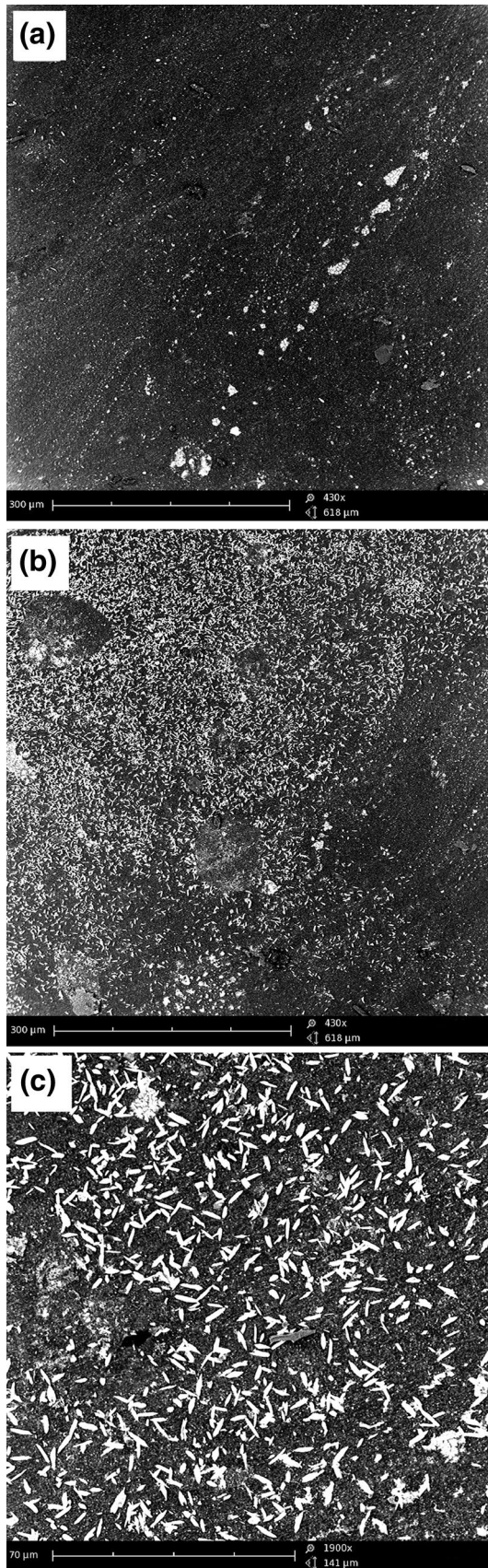


**Fig. 4** SEM micrographs of VNR45

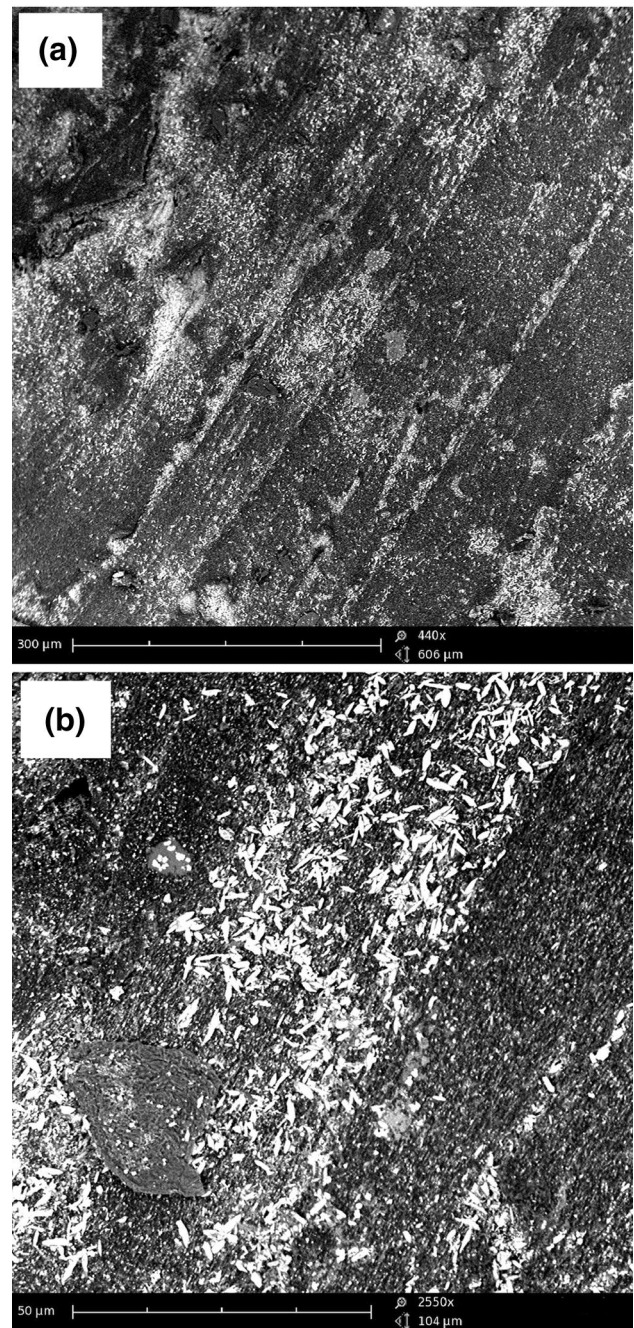


**Fig. 5** SEM micrographs of VNR85

elongation-at-break (984%) than natural rubber composites and the smallest tensile strength (in the case of compounds vulcanized in 10 min) in comparison with the prepared composites. The highest tensile strength value (21.2 MPa) was observed for the sample prepared using 15 parts of titanium dioxide per hundred parts of the natural rubber for the vulcanization time 10 min. The use of higher amounts of filler resulted in lowering of the tensile strength from 21.2 to 19.8 MPa for the vulcanization time of 10 min.

**Table 2** Effect of TiO<sub>2</sub> particles on swelling properties of the prepared composites

Sample code	Swelling ratio (SR) (%)	Volume fraction of a rubber network in the swollen phase ( $V_r$ )	Cross-link density ( $\nu$ ) $10^{-4}(\text{mol}/\text{cm}^3)$	Molecular weight of the polymer between cross-links ( $M_c$ ) (g/mol)
VNR	319.1 ± 1.7	0.2026 ± 0.0006	1.5847 ± 0.0114	6310 ± 45
VNR15	265.1 ± 5.5	0.2106 ± 0.0009	1.7312 ± 0.0170	5777 ± 56
VNR25	251.1 ± 0.7	0.2126 ± 0.0011	1.7481 ± 0.0217	5652 ± 69
VNR45	214.2 ± 0.5	0.2140 ± 0.0003	1.7967 ± 0.0066	5566 ± 20
VNR85	160.5 ± 1.1	0.2247 ± 0.0013	2.0114 ± 0.0270	4972 ± 66

**Table 3** Tensile strength and elongation-at-break of different composites samples vulcanized at 10 min

Sample code (-)	10 (min)		15 (min)		20 (min)		25 (min)	
	Tensile strength (MPa)	Elongation-at-break (%)	Tensile strength (MPa)	Elongation-at-break (%)	Tensile strength (MPa)	Elongation-at-break (%)	Tensile strength (MPa)	Elongation-at-break (%)
VNR	18.3 ± 0.5	984 ± 3	13.9 ± 0.2	932 ± 9	14.6 ± 1.0	973 ± 10	14.4 ± 0.6	981 ± 12
VNR15	21.2 ± 0.5	703 ± 15	18.5 ± 1.8	670 ± 7	16.8 ± 0.6	692 ± 12	14.1 ± 4.3	674 ± 24
VNR25	20.2 ± 0.2	691 ± 1	15.6 ± 0.2	676 ± 2	18.7 ± 0.1	734 ± 14	15.6 ± 0.8	778 ± 23
VNR45	20.1 ± 0.2	698 ± 2	17.1 ± 0.5	679 ± 6	12.2 ± 1.7	695 ± 26	14.4 ± 1.6	744 ± 11
VNR85	19.8 ± 1.2	681 ± 10	16.6 ± 3.7	652 ± 35	13.4 ± 0.1	663 ± 23	10.3 ± 2.3	634 ± 32

It was also found that optimal vulcanization time is equal 10 min, because higher vulcanization time resulted in decreasing of the tensile properties, e.g., in the case of VNR15 sample the tensile strength decreased from 21.2 MPa for 10 min to 14.1 MPa for 25 min vulcanization time. By use of 85 parts TiO<sub>2</sub>, tensile strength decreased to 10.3 MPa for samples vulcanized at 25 min. The similar trend was observed for elongation-at-break values. The reduction of mechanical properties when the vulcanization time was beyond 10 min, was connected with the reversion of the vulcanization process.

Similar results were obtained by Hayeemasae et al. [11] which prepared natural rubber composites at the loading of 0, 2, 4, 6, and 8 parts of TiO<sub>2</sub> particles per hundred parts of NR. Tensile strength and elongation-at-break decreased when the TiO<sub>2</sub> content was above six parts by weight per hundred parts of the rubber. They reported that using of nano-sized TiO<sub>2</sub> as filler for natural rubber composites resulted in better properties, as tensile modulus and tensile strength were more than those in the case of micro-sized TiO<sub>2</sub>-filled natural rubber composites [11].

This is resulted from better interaction between the NR matrix and the filler due to higher contact surface area between inorganic filler and polymer matrix, when nano-sized TiO<sub>2</sub> is used. The contact area between the filler and polymer matrix is one the important factor related to the obtain materials with improved properties. Addition of higher amounts of TiO<sub>2</sub> particles can causes agglomeration of filler due to filler–filler interactions. Furthermore,

the changes of tensile strength and elongation-at-break are sprightly connected with the dilution effect, and this is confirmed by other research works [11, 37].

The moduli at 100 and 300% elongation of the obtained composites are presented in Table 4. By increasing in the loading of TiO<sub>2</sub> in the obtained composites the moduli was increased. The natural rubber vulcanizates possess the smallest mentioned earlier moduli. The addition of TiO<sub>2</sub> caused reduction of elasticity, due to high hardness of introduced filler which resulted in more difficult deformation of material. Hayeemasae et al. [11] obtained similar results.

It is also known that moduli at 100 and 300% elongation are affected by the hardness of the fillers [28]. Moreover, with the increasing of vulcanization time the values of the mentioned moduli decreased. This is connected with the reversion of the vulcanization process, which is followed by increasing of the vulcanizates elasticity, and this fact is confirmed by the results of hardness and rebound resilience testing.

Many mechanisms of TiO<sub>2</sub> interactions in the natural rubber composites were described in detail by Hayeemasae et al. [11]. One of the main important factors is the possibility of aggregate formation. At the low content of TiO<sub>2</sub>, the good dispersion and lower amount of aggregates were achieved. The stress transfer rate is almost comparable with that in the case of unfilled rubber materials. A large amount of fillers caused the opposite behavior, and the stress transfer became ineffective due to the breakdown of the aggregates and the energy was absorbed by the rubber



**Table 4** Moduli at 100% and 300% of composites vulcanized at four different times

Vulcanized time (min)	10		15		20		25	
	M100 (MPa)	M300 (MPa)	M100 (MPa)	M300 (MPa)	M100 (MPa)	M300 (MPa)	M100 (MPa)	M300 (MPa)
VNR	0.88 ± 0.01	2.12 ± 0.02	0.75 ± 0.01	1.83 ± 0.02	0.72 ± 0.03	1.73 ± 0.03	0.71 ± 0.04	1.68 ± 0.02
VNR15	0.97 ± 0.01	2.39 ± 0.02	1.05 ± 0.04	2.69 ± 0.03	0.90 ± 0.01	2.17 ± 0.04	0.85 ± 0.01	2.04 ± 0.03
VNR25	1.07 ± 0.02	2.78 ± 0.01	0.99 ± 0.02	2.50 ± 0.04	0.98 ± 0.03	2.33 ± 0.02	0.78 ± 0.02	1.79 ± 0.01
VNR45	1.17 ± 0.03	3.16 ± 0.03	1.12 ± 0.04	2.97 ± 0.01	0.83 ± 0.01	2.11 ± 0.03	0.89 ± 0.02	2.21 ± 0.04
VNR85	1.49 ± 0.04	4.18 ± 0.04	1.49 ± 0.06	3.98 ± 0.05	1.17 ± 0.05	3.02 ± 0.04	1.05 ± 0.03	2.72 ± 0.07

chains on the filler surface [11]. All mentioned phenomena affect the mechanical properties of the prepared NR-based composites.

Improvement of polymer matrix composite properties depends on several factors, such as local polymer–filler interactions, filler–filler interactions and the geometry, size, dispersion and concentration of filler [25]. According to the literature, TiO<sub>2</sub> particles have large surface and improve interfacial interactions between fillers and NR matrix. It makes TiO<sub>2</sub> as reinforcing filler in the natural rubber composites [8, 11].

The mechanical properties of composites increase with the better dispersion of filler in the NR matrix. It should be pointed that by increase in the filler amount, the interactions between filler particles can be formed in addition to filler–polymer interactions. The titanium dioxide particles due to the presence of hydroxyl groups on their surfaces are hydrophilic. The presence of hydroxyl groups allow to form the hydrogen bonding between filler and NR which result in the formation of stronger interface. It contributes to an effective stress transfer and improving of the mechanical properties of TiO<sub>2</sub>/NR. The stronger bonding improves the wetting and adhesion of the polymer to the filler, due to the large surface area of filler. Furthermore, the smaller particle size of the filler is connected with the formation of better interfacial interactions between the inorganic filler and the polymer matrix [8, 25].

The improvement of the mechanical properties in the case of the composites filled with titanium dioxide was observed by several research groups. Esthappan et al. [38] found that in the case of polypropylene-based composites enhancement of the tensile strength and tensile modulus can be resulted from the interface formation between filler and polymer matrix, which can effectively transfer stress. The special interest is connected with TiO<sub>2</sub> nanoparticles which can improve the tensile and flexural properties, fracture toughness and impact energy, but the improvement of these properties depends strongly on the filler content in the composite [39].

Unfortunately, nanoparticles can form aggregates due to high interactions between particles (electrostatic Van der Waals forces) at high content of filler. Aggregates are

defects in the structure of composite, which are responsible for decreasing of the mechanical properties due to decreasing of contact area between the nanoparticles and polymer matrix [39, 40]. It is very important to obtain good dispersion of titanium dioxide particles in polymer matrix, because it results in a more uniform stress distribution in material and minimizes stress-concentration (like in the case of aggregates). Generally, the well dispersed filler results in the improvement of mechanical properties [39].

As was mentioned earlier the effectiveness of stress transfer between the natural rubber matrix and titanium dioxide particles is enhanced by the interaction of filler with polymer matrix. The relationship between the tensile strength of polymer composites and interfacial interactions was described by Pukanszky [41] and can be calculated using Eq. (3) as follows:

$$\sigma_c = \sigma_m \cdot \left( \frac{1 - V_p}{1 + 2.5 \cdot V_p} \right) \cdot e^{B \cdot V_p} \quad (3)$$

where,  $\sigma_c$  is the tensile strength of the prepared composites (i.e., VNR15, VNR25, VNR45 or VNR85),  $\sigma_m$  is the tensile strength of the polymer matrix (i.e., natural rubber vulcanizate without filler coded as VNR),  $V_p$  is the filler volume fraction (determined using the method presented by Leong et al. [42]), and  $B$  is the parameter related to the matrix–filler interactions.

The filler volume fractions and matrix–filler interaction parameters (calculated from Pukanszky relationship) for the prepared natural rubber composites filled with TiO<sub>2</sub> particles are presented in Table 5. The calculations were performed only for composites obtained at optimal vulcanization time, i.e., 10 min. The increase in the amount of TiO<sub>2</sub> particles (increase in filler volume fraction) in the prepared composites result in decreasing of matrix–filler interaction parameter resulted from the more filler–filler interactions which occurs due to the presence of hydroxyl groups on the surface of TiO<sub>2</sub> particles and formation of filler aggregates due to high interactions between the particles (as a result of electrostatic Van der Waals forces) at a high content of filler. Similar behavior was observed by Nath et al. [43] in the case of fly ash–isotactic polypropylene composites.

**Table 5** TiO<sub>2</sub> content effect in matrix–filler interaction parameter calculated from Pukanszky relationship

Sample code	Volume fraction of filler, $V_p$	Polymer matrix–filler interaction parameter, $B$
VNR15	0.028	8.53
VNR25	0.047	5.48
VNR45	0.082	4.46
VNR85	0.144	3.76

**Table 6** Tear strength values of composites vulcanized at different times

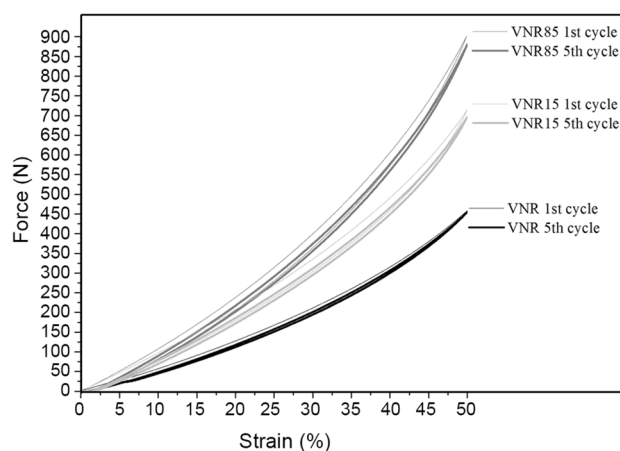
Vulcanized time (min)	10	15	20	25
Sample code	Tear Strength (N/mm)			
VNR	28.4 ± 0.8	20.7 ± 5.2	22.8 ± 3.0	23.6 ± 4.8
VNR15	33.6 ± 5.6	12.4 ± 3.7	10.6 ± 3.2	10.7 ± 3.5
VNR25	35.0 ± 5.6	8.4 ± 0.2	9.5 ± 1.1	11.6 ± 3.0
VNR45	30.9 ± 5.9	21.2 ± 6.7	7.7 ± 0.5	8.1 ± 0.6
VNR85	32.1 ± 3.5	25.5 ± 3.5	22.1 ± 2.5	21.4 ± 3.6

### Tear strength

Tear strength of the obtained rubber composites are presented in Table 6. The highest tear strength values were observed for the samples vulcanized at 10 min, and this also suggest that it is proper vulcanization time. Tear strength of all samples was increased with increase in TiO<sub>2</sub> loading up to 25 phr. The samples without filler exhibit the lowest tear strength values. This trend indicated a good interaction between filler surface with NR matrix, which resulted in cracks growth inhibition in the obtained rubber composites.

### Cyclic compression

The cyclic compression stress–strain curves for all prepared composites are shown in Fig. 6. The loading, unloading, dissipated energy values in each cycle and the difference between energy dissipated in the first and fifth cycle are presented in Table 7. The compression cycles were obtained until 50% compression. During compression–decompression (removing of loads) cycle, a certain amount of energy can be absorbed–released by the material. The use of higher amounts of filler caused increasing of energy dissipated from 0.075 to 0.181 J for the vulcanization time equal to 10 min. The lowest value of loading and unloading energy was observed for neat natural rubber vulcanizates. The loss of energy during each cycle is connected with the

**Fig. 6** First and fifth cycle compression stress–strain curves for VNR, VNR15, VNR85 at 10 min vulcanized time

deformation of the rubber matrix. It could be attributed to the interfacial interactions between TiO<sub>2</sub> and NR chains. The occurring interactions between polymer matrix and filler increased the work required for the deformation of the composites, because the energy is dissipated on the titanium dioxide particles. The addition of TiO<sub>2</sub> into soft matrix decreased the effectiveness of the stress transfer into rubber matrix and increased the work required to deform the composite. In all samples, permanent deformation at the end of their first cycle was observed, which indicated a change in the microstructure of the samples as a result of loading cycles and it mainly depended on the maximum strain level. This observation is also known from the literature [44].

### Abrasion resistance and density

The abrasion resistance and density of TiO<sub>2</sub>/NR vulcanizates are shown in Tables 8 and 9. The addition of TiO<sub>2</sub> to the rubber materials significantly improved the abrasion resistance. The lowest abrasion resistance was appeared in the natural rubber vulcanizates sample without TiO<sub>2</sub>. The values of the mentioned properties are strongly dependent on the amount of the used filler. The highest abrasion resistance for filled composites (0.024 cm<sup>3</sup>) was observed for sample VNR15 (vulcanization time of 10 min). The increase in loading of filler in the final material resulted in the lowering of abrasion resistance, but even in the TiO<sub>2</sub> content of 85 phr, the abrasion resistance was higher than that of the unfilled material. The increasing of the vulcanization time also resulted in decreasing of the abrasion resistance. The exceeding of the optimum vulcanization time is followed by regression of vulcanization process and thermal degradation of the obtained material, and consequently decreasing of the abrasion resistance.

**Table 7** Hysteresis characteristic of samples vulcanized for 10 min

Sample code	Cycle number	Loading energy $W_c$ (J)	Unloading energy $W_{RC}$ (J)	Dissipated energy $\Delta H$ (J)	$\Delta H_{1-5}$ (J)
VNR	1	2.225	2.093	0.132	0.075
	2	2.151	2.079	0.072	
	3	2.136	2.072	0.064	
	4	2.129	2.067	0.061	
	5	2.122	2.065	0.057	
VNR15	1	3.488	3.191	0.297	0.151
	2	3.324	3.150	0.174	
	3	3.284	3.125	0.158	
	4	3.259	3.108	0.151	
	5	3.238	3.093	0.146	
VNR85	1	4.218	3.886	0.333	0.181
	2	4.053	3.865	0.188	
	3	4.004	3.838	0.167	
	4	3.972	3.815	0.157	
	5	3.948	3.796	0.152	

**Table 8** Abrasion resistance of composites vulcanized at different times

Vulcanized time (min)	10	15	20	25
Sample code	Abrasion resistance ( $\text{cm}^3$ )			
VNR	$0.063 \pm 0.022$	$0.125 \pm 0.043$	$0.140 \pm 0.055$	$0.186 \pm 0.035$
VNR15	$0.024 \pm 0.004$	$0.035 \pm 0.011$	$0.037 \pm 0.003$	$0.051 \pm 0.010$
VNR25	$0.035 \pm 0.003$	$0.035 \pm 0.001$	$0.054 \pm 0.007$	$0.054 \pm 0.005$
VNR45	$0.037 \pm 0.002$	$0.041 \pm 0.003$	$0.059 \pm 0.003$	$0.071 \pm 0.010$
VNR85	$0.033 \pm 0.023$	$0.053 \pm 0.001$	$0.055 \pm 0.005$	$0.071 \pm 0.004$

**Table 9** Density of composites vulcanized at different times

Vulcanized time (min)	10	15	20	25
Sample code	Density ( $\text{g cm}^{-3}$ )			
VNR	$0.9679 \pm 0.0001$	$0.9677 \pm 0.0034$	$0.9641 \pm 0.0035$	$0.9665 \pm 0.007$
VNR15	$1.0678 \pm 0.0022$	$1.0644 \pm 0.0006$	$1.0654 \pm 0.0004$	$1.0645 \pm 0.0004$
VNR25	$1.1182 \pm 0.0003$	$1.1184 \pm 0.0003$	$1.1184 \pm 0.008$	$1.1177 \pm 0.0003$
VNR45	$1.2264 \pm 0.0003$	$1.2276 \pm 0.0005$	$1.2255 \pm 0.0001$	$1.4163 \pm 0.0005$
VNR85	$1.4163 \pm 0.0005$	$1.4161 \pm 0.0006$	$1.4167 \pm 0.0004$	$1.4168 \pm 0.0007$

Density of the produced composites is in the range  $1.0678\text{--}1.416 \text{ g cm}^{-3}$  and density of the unfilled natural rubber vulcanizates is  $0.9679 \text{ g cm}^{-3}$ . As is shown in Table 9, density values of the obtained composites were increased with the increase in the loading titanium dioxide resulted from higher density of  $\text{TiO}_2$  particles in comparison with the vulcanized natural rubber. The smallest density was observed for natural rubber with 15 parts per titanium dioxide per hundred parts of natural rubber. Generally, it was observed that the densities of materials are very similar and independent of the vulcanization time.

### Hardness and rebound resilience

The hardness and rebound resilience of the obtained materials are presented in Table 10. The results were depended on the content of titanium dioxide and vulcanization time. Hardness of the samples was in the range of  $46.4\text{--}54.3^\circ\text{ShA}$  for 10 min vulcanization time. It was also found that optimal vulcanization time was 10 min, because higher vulcanization time resulted in decreasing of the hardness and rebound resilience. The natural rubber vulcanizates without filler possessed the smallest hardness and with

**Table 10** Hardness and rebound resilience of composites vulcanized at four different times

Vulcanized time (min)	10		15		20		25	
	Hardness (°Sh A)	Rebound resilience (%)	Hardness (°Sh A)	Rebound resilience (%)	Hardness (°Sh A)	Rebound resilience (%)	Hardness (°Sh A)	Rebound resilience (%)
VNR	39.7 ± 0.9	43.8 ± 2.1	37.5 ± 0.2	41.2 ± 1.6	36.8 ± 0.4	40.2 ± 1.9	36.0 ± 0.4	39.4 ± 2.0
VNR15	46.4 ± 0.6	50.3 ± 3.1	45.6 ± 0.3	49.0 ± 2.6	44.9 ± 0.8	51.1 ± 4.3	43.1 ± 0.8	51.2 ± 2.3
VNR25	46.5 ± 1.8	52.1 ± 2.4	46.2 ± 0.3	52.0 ± 2.7	44.6 ± 0.3	48.0 ± 2.8	43.6 ± 0.5	47.8 ± 2.7
VNR45	50.2 ± 0.3	49.9 ± 2.7	46.8 ± 1.0	49.9 ± 2.5	44.9 ± 1.0	46.6 ± 2.9	44.4 ± 0.6	45.7 ± 2.1
VNR85	54.3 ± 0.5	50.5 ± 2.0	52.9 ± 0.7	47.4 ± 2.1	51.2 ± 0.3	45.7 ± 2.5	49.5 ± 0.3	43.5 ± 2.1

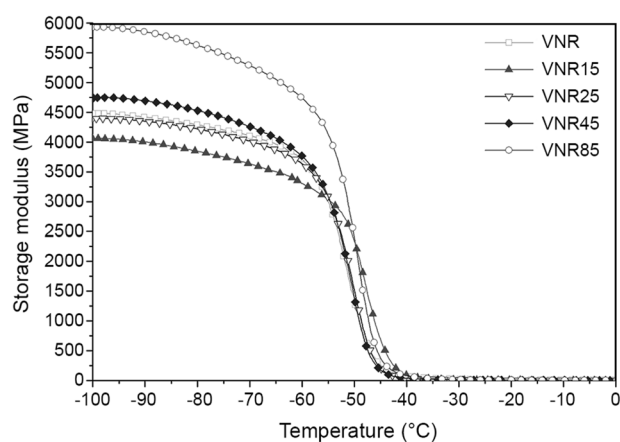
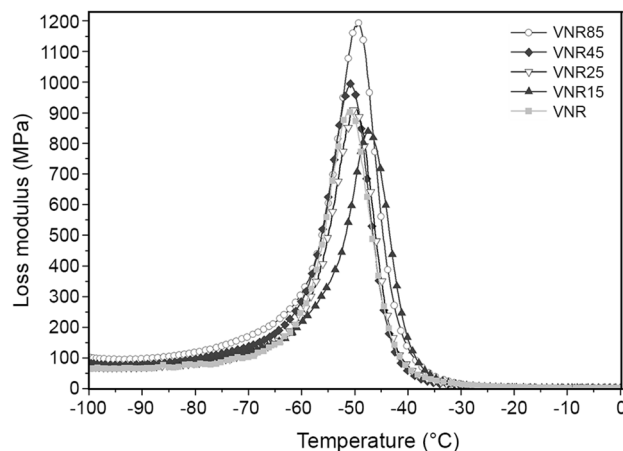
increase in the loading of the filler, hardness was enhanced. Therefore, the highest hardness (54.3°ShA) was observed for the sample with 85 parts per titanium dioxide hundred parts of natural rubber.

When the vulcanization time increased the cure time, hardness of the prepared rubber vulcanizates decreased. As stated above, the increasing of the vulcanization time resulted in thermal degradation of the composites and decreasing their hardness. The rebound resilience was in the range 43.5–52.9% and vulcanization time-independent. It can be concluded that the rebound resilience was depended strongly on the filler distribution in the elastomeric matrix. It can be concluded that results were dependent on the places, where the pendulum fall on the sample. When the pendulum hit on the surface where the large agglomerates were present, filler received energy of impact and this resulted in the lower rebound resilience than when the pendulum hit on the elastomeric surface.

### Dynamic mechanical thermal analysis

Results from dynamic mechanical thermal analysis (DMTA) of the prepared composites are shown in Figs. 7, 8, 9. In the temperature range from  $-100$  to  $0$  °C, the natural rubber composites have generally higher storage modulus ( $E'$ ) in comparison with the neat natural rubber vulcanizates. As can be seen in Fig. 7 use of 85 parts  $\text{TiO}_2$  per hundred parts of natural rubber significantly increased the storage modulus in the glassy region, which is connected with the enhancement of composite stiffness due to the presence of the inorganic filler characterized by high hardness.

In the Fig. 8, loss modulus ( $E''$ ) dependence on temperature for all prepared materials is presented. Loss modulus of composites is in the range of 846–1200 MPa. Generally, the maximum value of the loss modulus increased with increase in the amount of filler content, which is connected with higher loss energy. The glass transition temperature is determined as a temperature at which  $\tan\delta$  reaches its maximum value. The tangent delta dependence on the

**Fig. 7** Storage modulus changes vs. temperature of different composites samples vulcanized at 10 min**Fig. 8** Loss modulus changes vs. temperature of different composites samples vulcanized at 10 min

temperature (Fig. 10; Table 11) for natural rubber composites showed that the height of  $\tan\delta$  peak is affected by the amount of filler.

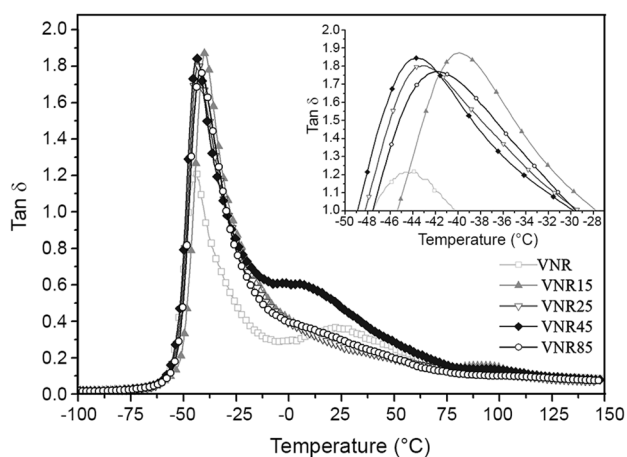


**Fig. 9** Temperature dependence of  $\tan\delta$  of different composite samples vulcanized at 10 min

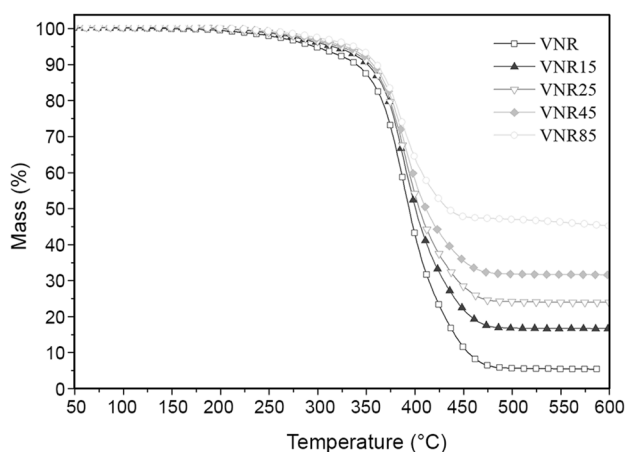


**Fig. 10** TGA curves of different composite samples and reference sample

### Thermogravimetric analysis

Thermal stability of the prepared natural rubber composites are shown in Figs. 10 and 11 (TGA and DTG curves). The characteristic temperatures of thermal decomposition are presented in Table 12. As can be seen thermal degradation of VNR begins at 200 °C. All natural rubber composites showed a one stage thermal degradation. It is evident that the highest thermal stability is exhibited by VNR85. In Fig. 11, it is also discernible the existence of one stage thermal decomposition for all materials. The highest rate of thermal decomposition was observed at ca. 390 °C for all prepared materials. Addition of  $\text{TiO}_2$  particles to NR resulted in the increase of thermal stability, which was due to the high thermal stability of the applied inorganic

**Table 11** Glass transition temperature of the obtained composites determined by DMA method

Sample code	$T_g$ (°C)	$\tan\delta$
VNR	-44.5	1.21
VNR15	-40.0	1.87
VNR25	-43.0	1.81
VNR45	-43.6	1.84
VNR85	-42.0	1.77

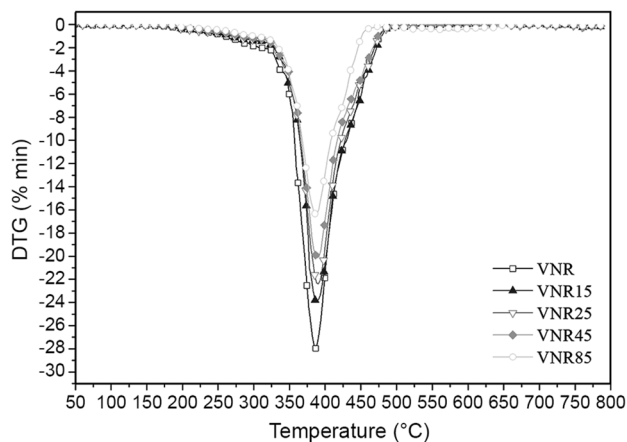


**Fig. 11** DTG curves of different composite samples and reference sample

filler. The incorporation of titanium dioxide can improve the mechanical properties and thermal stability of the prepared composites. It is also observable that the maximum degradation temperature for the composites filled with 85 parts  $\text{TiO}_2$  by weight per hundred parts of rubber is slightly higher than the other samples. Natural rubber composites showed higher thermal stability than the neat natural rubber vulcanizates. The char yield at 600 °C is in the good correlation with the percentage weight content of titanium dioxide in the prepared composites (Tables 1, 11).

The improvement of the thermal stability of the polymer matrix composites can be obtained by the presence of fillers (e.g.,  $\text{TiO}_2$  particles) which can interact with the polymer matrix. The relatively strong interactions between the filler surfaces and polymer chains resulted in restriction of thermal movements (mobility) of polymer chains [38]. Esthappan et al. [45] suggested that in the case of polypropylene composites filled with  $\text{TiO}_2$  particles, the good interfacial interactions restricted the mobility of the polymer chains and made the scission of polymer harder, and due to this reasons the degradation temperature is shifted to the higher temperatures.

**Table 12** Thermal stability of the obtained composites

Sample code	$T_5$ (°C)	$T_{10}$ (°C)	$T_{30}$ (°C)	$T_{50}$ (°C)	$T_{max}$ (°C)	Char yield at 600 °C (%)
VNR	294.4	339.5	376.9	394.5	386.9	5.4
VNR15	313.2	350.7	383.2	400.7	387.9	16.3
VNR25	322.1	352.1	384.6	404.6	389.3	23.5
VNR45	327.8	355.3	387.8	412.8	389.7	31.2
VNR85	336.6	359.1	391.7	434.2	387.3	44.3

## Conclusion

The results showed that using titanium dioxide as filler allows obtaining materials with improved mechanical properties and thermal stability in comparison with the neat natural rubber vulcanizates. Prepared natural rubber composites exhibited higher tensile strength, hardness, moduli at 100 and 300% elongation, and abrasion resistance than the unfilled natural rubber vulcanizates. SEM analysis showed generally good dispersion of the filler in the elastomeric matrix. However, inorganic filler at higher loadings showed ability to form agglomerates, which are responsible for decrease of mechanical properties. It was generally observed that even with decline in mechanical properties by increase in  $TiO_2$  contents, the obtained values from mechanical tests were higher than those in the case of the unfilled natural rubber. Moreover, composites with 85 phr of titanium dioxide have surprisingly good mechanical properties and thermal stability. Titanium dioxide as a filler has a very good potential for production new materials with better mechanical properties and thermal stability in comparison with the neat natural rubber vulcanizates. This kind of material is a good candidate for specific applications, e.g., rubber outsoles for footwear, due to some suitable properties, including good abrasion resistance and flexibility, white color, antimicrobial properties and attenuation of ultraviolet light (UV protection) connected with the presence of titanium dioxide particles. The further investigations (in the terms of specific industrial standards) should be performed before the application of this kind of materials.

## Compliance with ethical standards

**Conflict of interest** The authors declare that they have no conflict of interest.

**Open Access** This article is distributed under the terms of the Creative Commons Attribution 4.0 International License (<http://creativecommons.org/licenses/by/4.0/>), which permits unrestricted use, distribution, and reproduction in any medium, provided you give appropriate credit to the original author(s) and the source, provide a link to the Creative Commons license, and indicate if changes were made.

## References

- Zhong B, Jia Z, Luo Y, Jia D (2015) A method to improve the mechanical performance of styrene-butadiene rubber via vulcanization accelerator modified silica. *Compos Sci Technol* 117:46–53
- Le HH, Sriharish MN, Henning S, Klehm J, Menzel M, Frank W, Wießner S, Das A, Stöckelhuber KW, Heinrich G, Radusch HJ (2014) Dispersion and distribution of carbon nanotubes in ternary rubber blends. *Compos Sci Technol* 90:180–186
- Hosseini SM, Razzaghi-Kashani M (2014) Vulcanization kinetics of nano-silica filled styrene butadiene rubber. *Polymer* 55:6426–6434
- Tangudom P, Thongsang S, Sombatsompop N (2014) Cure and mechanical properties and abrasive wear behavior of natural rubber, styrene-butadiene rubber and their blends reinforced with silica hybrid fillers. *Mater Des* 53:856–864
- Bellucci FS, Lobato de Almeida FC, Lima Nobre MA, Rodríguez-Pérez MA, Paschoalinia AT, Job AE (2016) Magnetic properties of vulcanized natural rubber nanocomposites as a function of the concentration, size and shape of the magnetic fillers. *Compos Part B-Eng* 85:196–206
- Ali Shah A, Hasan F, Shah Z, Kanwal N, Zeb S (2013) Biodegradation of natural and synthetic rubbers: a review. *Int Biodeter Biodegr* 83:145–157
- Ozbay S, Erbil HY (2015) Superhydrophobic and oleophobic surfaces obtained by graft copolymerization of perfluoroalkyl ethyl acrylate onto SBR rubber. *Colloids Surf A* 481:537–546
- Seentrakoon B, Junhasavasdikul B, Chavasiri W (2013) Enhanced UV-protection and antibacterial properties of natural rubber/rutile- $TiO_2$  nanocomposites. *Polym Degrad Stabil* 98:566–578
- Ismail M, Abd El Ghaffar M, Shaffei K, Mohamed N (1999) Some novel polyamines as antioxidants for SBR vulcanizates. *Polym Degrad Stabil* 63:377–383
- Erdem N, Erdogan UH, Cireli AA, Onar N (2010) Structural and ultraviolet-protective properties of nano- $TiO_2$ -doped polypropylene filaments. *J Appl Polym Sci* 115:152–157
- Hayeemasae N, Rathnayake WGIU, Ismail H (2015) Nano-sized  $TiO_2$ -reinforced natural rubber composites prepared by latex compounding method. *J Vinyl Addit Technol*. doi:10.1002/vnl.21497
- Nabil H, Ismail H, Rashid AA (2012) Effects of partial replacement of commercial fillers by recycled poly(ethylene terephthalate) powder on the properties of natural rubber composites. *J Vinyl Addit Technol* 18:139–146
- Prasertsri S, Rattanasom N (2011) Mechanical and damping properties of silica/natural rubber composites prepared from latex system. *Polym Test* 30:515–526
- Li Y, Han B, Liu L, Zhang F, Zhang L, Wen S, Lu Y, Yang H, Shen J (2013) Surface modification of silica by two-step method and properties of solution styrene butadiene rubber (SSBR) nanocomposites filled with modified silica. *Compos Sci Technol* 88:69–75



15. Zhong B, Jia Z, Hu D, Luo Y, Jia D (2015) Reinforcement and reinforcing mechanism of styrene–butadiene rubber by antioxidant-modified silica. *Compos Part A-Appl S* 78:303–310
16. Cao X, Xu C, Liu Y, Chen Y (2013) Preparation and properties of carboxylated styrene-butadiene rubber/cellulose nanocrystals composites. *Carbohydr Polym* 92:69–76
17. Nasu A, Otsubo Y (2007) Rheology and UV-protecting properties of complex suspensions of titanium dioxides and zinc oxides. *J Colloid Interf Sci* 310:617–623
18. Jin M, Zhang X, Emeline AV, Numata T, Murakami T, Fujishima A (2008) Surface modification of natural rubber by TiO<sub>2</sub> film. *Surf Coat Tech* 202:1364–1370
19. Zhang Q, Tian M, Wu Y, Lin G, Zhang L (2004) Effect of particle size on the properties of Mg(OH)<sub>2</sub>-filled rubber composites. *J Appl Polym Sci* 94:2341–2346
20. Rathnayake WGIU, Ismail H, Baharin A, Darsanasiri AGND, Rajapakse S (2012) Synthesis and characterization of nano silver based natural rubber latex foam for imparting antibacterial and anti-fungal properties. *Polym Test* 31:586–592
21. Zhou Y, Fan M, Chen L, Zhuang J (2015) Lignocellulosic fibre mediated rubber composites: an overview. *Compos Part B-Eng* 76:180–191
22. Ahmed K, Nizami SS, Raza NZ, Habib F (2013) The effect of silica on the properties of marble sludge filled hybrid natural rubber composites. *J King Saud Univ Sci* 25:331–339
23. Ahmed K, Nizami SS, Riza NZ (2014) Reinforcement of natural rubber hybrid composites based on marble sludge/Silica and marble sludge/rice husk derived silica. *J Adv Res* 5:165–173
24. Jong L (2015) Influence of protein hydrolysis on the mechanical properties of natural rubber composites reinforced with soy protein particles. *Ind Crop Prod* 65:102–109
25. Ochigbo SS, Luyt AS (2012) Mechanical and morphological properties of films based on ultrasound treated titanium dioxide dispersion/natural rubber latex. *Int J Compos Mater* 1:7–13
26. Kikuchi Y, Sunada K, Iyoda T, Hashimoto K, Fujishima A (1997) Photocatalytic bactericidal effect of TiO<sub>2</sub> thin films: dynamic view of the active oxygen species responsible for the effect. *J Photochem Photobiol A* 106:51–56
27. Meera AP, Said S, Grohens Y, Luty AS, Thomas S (2009) Tensile stress relaxation studies of TiO<sub>2</sub> and nanosilica filled natural rubber composites. *Ind Eng Chem Res* 48:3410–3416. doi:10.1021/ie801494s
28. Fu SY, Feng XQ, Lauke B, Mai YW (2008) Effects of particle size, particle/matrix interface adhesion and particle loading on mechanical properties of particulate–polymer composites. *Compos Part B-Eng* 39:933–961
29. Wang Z, Lu Y, Liu J, Dang Z, Zhang L, Wang W (2011) Preparation of nano-zinc oxide/EPDM composites with both good thermal conductivity and mechanical properties. *J Appl Polym Sci* 119:1144–1155
30. Das A, Stöckelhuber KW, Jurk R, Saphiannikova M, Fritzsche J, Lorenz H, Klüppel M, Heinrich G (2008) Modified and unmodified multiwalled carbon nanotubes in high performance solution-styrene–butadiene and butadiene rubber blends. *Polymer* 49:5276–5283
31. Ahmed K, Nizami SS, Raza NZ, Mahmood K (2012) Mechanical, swelling, and thermal aging properties of marble sludge-natural rubber composites. *Int J Ind Chem* 3:1–12
32. Datta J, Wloch M (2016) Preparation, morphology and properties of natural rubber composites filled with untreated short jute fibres. *Polym Bull*. doi:10.1007/s00289-016-1744-x
33. Manaila E, Stelescu MD, Doroftei F (2015) Polymeric composites based on natural rubber and hemp fibers. *Iran Polym J* 24:135–148
34. Delor F, Barrois-Oudin N, Duteurtre X, Cardinet C, Lemaire J, Lacoste J (1998) Oxidation of rubbers analysed by HATR/IR spectroscopy. *Polym Degrad Stabil* 62:395–401
35. Dhandapani S, Nayak SK, Mohanty S (2015) Compatibility effect of titanium dioxide nanofiber on reinforced biobasednanocomposites: thermal, mechanical, and morphology characterization. *J Vinyl Addit Technol*. doi:10.1002/vnl.21475
36. Sikong L, Masae M, Kooptarnond K, Taweepreda W, Saito F (2012) Improvement of hydrophilic property of rubber dipping former surface with Ni/B/TiO<sub>2</sub> nano-composite film. *Appl Surf Sci* 258:4436–4443. doi:10.1016/j.apsusc.2012.01.002
37. Poompradub S, Ikeda Y, Kokubo Y, Shiono T (2008) Cuttlebone as reinforcing filler for natural rubber. *Eur Polym J* 44:4157–4164
38. Esthappan SK, Kuttappan SK, Joseph R (2012) Effect of titanium dioxide on the thermal ageing of polypropylene. *Polym Degrad Stabil* 97:615–620
39. Pinto D, Bernardo L, Amaro A, Lopes S (2015) Mechanical properties of epoxy nanocomposites using titanium dioxide as reinforcement—a review. *Constr Build Mater* 95:506–524
40. Hanemann T, Szabó DV (2010) Polymer-nanoparticle composites: from synthesis to modern applications. *Materials* 3:3468–3517
41. Pukánszky B (1990) Influence of interface interaction on the ultimate tensile properties of polymer composites. *Composites* 21:255–262
42. Leong YW, AbuBakar MB, Mohd Ishak ZA, Ariffin A, Pukánszky B (2004) Comparison of the mechanical properties and interfacial interactions between talc, kaolin, and calcium carbonate filled polypropylene composites. *J Appl Polym Sci* 91:3315–3326
43. Nath DCD, Bandyopadhyay S, Yu A, Zeng Q, Das T, Blackburn D, White C (2009) Structure–property interface correlation of fly ash–isotactic polypropylene composites. *J Mater Sci* 44:6078–6089
44. Kim W, Argento A, Flanigan C, Mielewski DF (2015) Effects of soy-based oils on the tensile behavior of EPDM rubber. *Polym Test* 46:33–40
45. Esthappan SK, Kuttappan SK, Joseph R (2012) Thermal and mechanical properties of polypropylene/titanium dioxide nanocomposite fibers. *Mater Des* 37:537–542